Impact Assessment of Wheeling Renewable Distributed Generation to Residential Load

Abdullahi Baba Abdullahi
Department of Electrical and Electronic Engineering
Federal University of Technology
Minna, Nigeria
wangwaeeee@gmail.com

Lanre Olatomiwa
Department of Electrical and Electronic Engineering
Federal University of Technology
Minna, Nigeria
olatomiwa.l@futminna.edu.ng

Jacob Tsado
Department of Electrical and Electronic Engineering
Federal University of Technology
Minna, Nigeria
tsadojacob@futminna.edu.ng

Ahmad Abubakar Sadiq
Department of Electrical and Electronic Engineering
Federal University of Technology
Minna, Nigeria
ahmad.abubakar@futminna.edu.ng

Abstract— With a national peak demand forecast of 28,850 megawatt, against the grid generation installed capacity of 13,014.14 megawatt, the Nigeria electricity consumers suffer from an inadequate and unstable supply. The residential sector, which accounts for about 60 % of electricity consumption, is the worst hit. An alternate electricity supply system capable of addressing this problem is energy wheeling, which entails delivering electricity generated by an independent power producer to residential consumers via the grid distribution network under a power purchase agreement. The aim of this paper is to determine the technical impact of transporting distributed generation from solar and wind energy resources, to residential load of Gwarinpa housing estate (GHE), Abuja, Nigeria. Two software packages; Hybrid optimization for multiple energy resources (HOMER) and digital simulation of electrical networks (DIgSILENT), were used to determine the renewable energy potential for the estate and the impact of wheeling on voltage profile, fault level, power losses and thermal loading of the distribution network respectively. Unlike wind energy that showed no potential, with an average wind speed of 3.01 m/s at a hub height of 50m, solar resource showed good potential with an annual average of the daily solar radiation of 5.55 kWh/m^2/day. The result also produced a net present cost of 72.4 million USD and the lowest cost of energy of 0.0188 USD/kWh.

Keywords—Nigeria, residential electricity consumers, energy wheeling, solar and wind renewable energy, Distributed Generation, HOMER, DIgSILENT.

I. INTRODUCTION

Nigeria, with a population estimate of over 208 million [1], is the most populated country in Africa. With population being a key indicator of electricity consumption [2], it is not unexpected that Nigeria national peak demand forecast, estimated at 28,850 megawatt (MW), creates a huge gap with the generating capacity of 7,652 MW. Thus, the Nigeria electricity supply industry (NESI) is characterized by gross supply inadequacy and incessant power cuts. During power cuts, consumers resort to self-generation mostly from diesel generating sets and bear the associated burden and challenges. With an estimate of over 60 % of electricity consumption [3], residential electricity consumers are the worst hit. Recent measures taken by the government to reverse the trend includes deregulation of the power sector. The energy power reform act of 2005 was passed, and the erstwhile state-owned power holding company of Nigeria (PHCN) lost its monopoly. A new NESI emerged, including private investors in power generation and distribution. As the deregulation gets entrenched, the future NESI would be characterized by a paradigm shift from central to distributed generation (DG) mostly from renewable resources.

Energy wheeling, an alternative electricity supply system from independent power producers (IPP), would be available for consumers via the existing grid network, under power purchase agreement [4]. During energy wheeling, the grid distribution network parameters could be distorted with the integration of DG [5]. The case study, Gwarinpa housing estate Abuja is the largest residential estate in Nigeria with a load consumption of about 30 MW. Power is supplied to the estate from two transmission substations and three distribution substations via a 9-bus distribution network.

In this paper, HOMER software was used to determine the potential for solar and wind energy resources around the case study. The result showed good potential with an annual average of the daily solar radiation of 5.55 kWh/m^2/day. On the other hand, the low wind speed of 3.01 m/s obtained shows no wind energy potential. Furthermore, the impact of wheeling renewable DG to loads of residential characteristics on the voltage profile, fault level, power losses and thermal loading of the existing grid distribution network was determined. Similarly, the impact of distance between the DG sites and the load on these distribution network parameters was determined. Furthermore, comparisons were made between the results of the grid distribution network and the DG connected distribution network.

II. REVIEW OF RELATED WORKS

Several research has been conducted to find solutions to challenges associated with renewable energy resource exploration and utilization impact assessment.

A study was carried out on a distribution network that supplies two industrial loads in South Africa, and a comparison was made with a network powered by a DG using HOMER and DIgSILENT simulation software [4]. Solar and wind resources with global horizontal irradiance (GHI) levels exceeding 2200 kWh/m^2 and wind speeds of 8 m/s at 100 m above sea level, respectively, were shown to have greater potential. . With levelized cost of electricity (LCOE) at 0.065

$/kWh for 16 MW and 0.063 $/kWh for 70 MW, the wind energy was financially more viable. Furthermore, the size of DG was directly proportional to fault contribution to the network fault level. Both the line losses and the equipment thermal loading were affected by the distance between the DG and the load [4].

To improve reliability of electricity supply to Ethiopian industrial parks, three industrial sites were considered for study using HOMER Pro [6]. The grid/diesel/PV/wind/battery system was obtained as the most viable of the different scenarios analyzed. The cost of energy were 0.044, 0.049 and 0.048 $/kWh. CO_2 emission reduced by 45 %, 44 % and 42 %

In a similar study conducted by [7] Al Ghaithi *et.al,* on an off-grid hybrid energy system in Masira Island, Oman, a diesel-powered network of 20.3 MW was comparatively analyzed with diesel-PV and diesel-PV-Wind hybrid systems. HOMER and DIgSILENT software were used, and the most economically viable scenario was the diesel-PV-Wind hybrid, with a 7 % reduction in NPC. The LCOE was 0.272 $/kWh, and the impact of load distance on the voltage profile at the 11 kV and 33 kV feeders was significant. The lowest voltage of 0.85p.u, a significant drop of 15 %, was recorded on the farthest bus. However, with the introduction of PV, reduction in line load and increase in voltage to 0.98p.u were obtained.

The impact of PV systems voltage profile and power losses of 33 kV distribution networks in Al-Mafraq, Jordan was studied and analyzed by [8] using DIgSILENT. Salhyia 33 kV feeder of 7 MW connected to a PV system of 3 MW produced a network with declining voltage as the distance from the source increases. A range of 0.98 p.u and 0.94 p.u was obtained and subsequently improved to the least value of 0.95 p.u after PV integration. Similarly, power losses were significantly minimized from 7.01 % to 3.82 % before and after PV integration, respectively. Similar results were obtained from studies conducted by [5, 9].

In a related study, a nano-grid was designed for the residential load of five households in Danladi Nasidi quarters, Kano, Nigeria [10]. HOMER optimization was carried out to analyze the PV, wind turbine and storage system with a 24 hours load demand. The result of the most viable optimal configuration had 150 kW, 4500 kW and 130 kW PV capacity, wind turbine and inverter components, respectively.

III. DISTRIBUTED GENERATION AND THE DISTRIBUTED NETWORK PARAMETERS

The integration of distributed generation to the existing grid distribution network altars the flow of power [4, 5]. As a result, network parameters like voltage profile, fault level, losses, and thermal loading characteristics are distorted.

A. Voltage Profile

Voltage drop occurs between the source and the load, and as the distance increases, voltage drop becomes significant [4]. The line impedance and the quantity of load current accounts for the loss. Integration of DG to the network system provides additional capacity and thus, improves the voltage profile.

In a two-bus distribution line shown in Figure 1 [4], the voltage drop is illustrated by equations (2), (3) and (4).
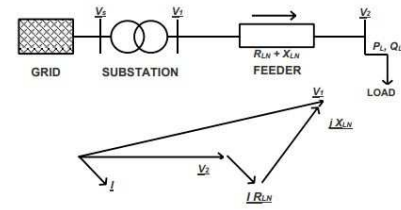

Fig. 1. Voltage drop in a two-bus distribution line with corresponding phasor diagram [4]

The current $\underline{I}$ is given by the following expression:

$$I = \frac{S}{V_2} = \frac{PL - jQL}{V_2} \qquad (1)$$

where $\underline{S}$ is the apparent power at the voltage $\underline{V}_2$, V_S is the transformer primary voltage (V), V_1 is the transformer secondary voltage (V), V_2 is the load bus voltage (V), P is the active power flow (W), Q is the reactive power flow (var), P_L is the active power at the load (W), Q_L is the reactive power at the load (var)

The drop in voltage is given by,

$$V_1 - V_2 = I\left(R_{LN} + jX_{LN}\right)$$
$$= R_{LN}P_L + X_{LN}Q_L - \frac{j(X_{LN}P_L - R_{LN}Q_L)}{V_2} \qquad (2)$$

The voltage angle $V_1 - V_2$ is small, for small voltage flow. Thus, the imaginary part of (2) can be neglected. Therefore, the voltage drop becomes:

$$\Delta V \approx \frac{R_{LN}P_L + X_{LN}Q_L}{V_2} \qquad (3)$$

With DG connected to the two-bus distribution line shown in Fig. 2 [4].
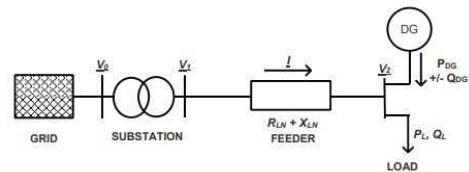

Fig. 2.   The DG connected two-bus distribution line [4].

The voltage drop is expressed as follows:
$$\Delta V = V_1 - V_2 \approx R_{LN}(P_L - P_{DG}) + X_{LN}(Q_L - (\pm Q_{DG})/V_2 \qquad (4)$$

Where P_{DG} is the active power generated by the DG and Q_{DG} is the reactive power generated by the DG.

B. Fault Level

Faults in power systems could be caused by equipment failure, maloperation, and natural phenomena such as thunder, tornadoes and so on. The integration of DG contributes to the system fault level, depending on the type, size, mode of connection and fault distance. The equivalent voltage source

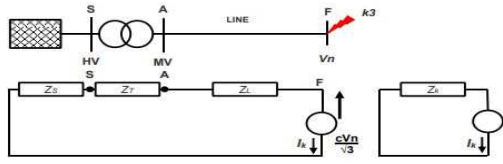is used to illustrate the three-phase symmetrical short circuit current in Fig. 3.

Fig. 3.   The symmetrical short circuit current using equivalent voltage source [4].

Using the equivalent voltage source, the three-phase symmetrical short circuit current is given as:

$$I_K = \frac{cVn}{\sqrt{3}Z_K} = \frac{cVn}{\sqrt{3}(Z_T + Z_L + Z_S)} \qquad (5)$$

Where Z_K is the equivalent short circuit impedance of the network at the fault location (Ω), Z_S = network impedance (Ω), Z_T = transformer impedance (Ω) and Z_L = load impedance (Ω).

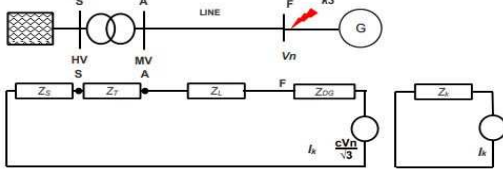The DG connected network is shown in Fig. 4 [4].

Fig. 4.   The symmetrical short circuit current of DG connected network using equivalent voltage source [4].

The short circuit current is expressed as:

$$I_K = \frac{cVn}{\sqrt{3}Z_K} = \frac{cVn}{\sqrt{3}(Z_S + Z_T + Z_L + Z_{DG})} \qquad (6)$$

where Z_{DG} = equivalent impedance of the DG (Ω)

C. Line Losses

Line losses are a function of the line resistance and the magnitude of current flowing in the circuit. Integrating DG to the network mitigates against the loss by minimizing the magnitude of current flow at and close to the connected network. The line losses in a distribution network is expressed as [4]:

$$P_{loss} = 3 \times I_L^2 \times R \times L \qquad (7)$$

Where P_{loss} is the line losses (W), R is the line resistance (Ω), L is the substation to load distance in km, I_L is the line current (A).

With DG connected to the network, the total network losses are the sum of network losses between the substation and DG and network losses between the load and DG. The losses between the substation and DG is given as:

$$P_{loss(SDG)} = \frac{R \times G}{3V_L^2}(P_L^2 + Q_L^2 + P_G^2 + Q_G^2 + 2P_L P_G - 2Q_L Q_G) \quad (8)$$

Thus, the losses between the load and DG is expressed as,

$$P_{loss(LDG)} = \frac{R \times L}{3V_L^2}$$
$$= \left[(P_L^2 + Q_L^2) + (P_G^2 + Q_G^2 - 2P_L P_G - 2Q_L Q_G)\left(\frac{G}{L}\right) \right] \qquad (9)$$

Therefore, the total network loss is expressed as [4]

$$P_{Tloss} = \frac{R \times (P_L^2 + Q_L^2)}{3V_L^2}(L - G) \qquad (10)$$

Where P_L is the active power of load (W), P_G is the active power of DG (W), Q_L is the reactive power of load (var), Q_G is the reactive power of DG (var), V_L is the load voltage (V), G is the distance between the substation and DG (km), L is the distance between the load and DG (km).

D. Thermal Loading

Power system equipment is designed to operate under certain specifications, such as the current-carrying capability. Beyond the design limit, equipment may be overloaded, leading to excessive rise in temperature and eventual breakdown of insulation. Integrating DG provides additional capacity that could relieve overload.

IV.   THE CASE STUDY

The distribution network that supplies power to Gwarinpa residential estate, modelled in DIgSILENT, is shown in Fig. 5.
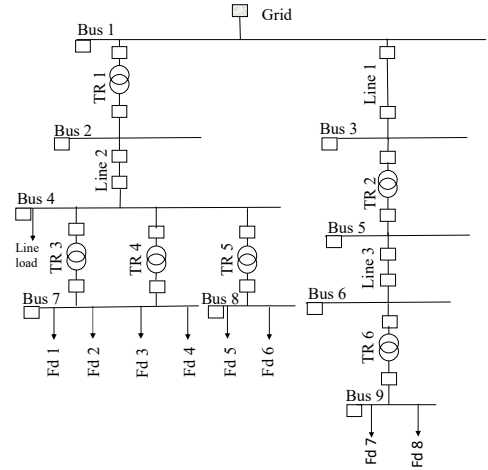

Fig. 5.   The distribution network system designed in DIgSILENT.

The network, energized by a 330/132 kV Substation, consists of a 132 kV busbar which feeds two 132 kV transmission substations located at Katampe and Kubwa via (line 1). The Katampe substation has a 60 MVA, 132/33 kV transformer that feeds GHE via a 33 kV Gwarinpa feeder (Line 2). The feeder, about 15 km to GHE, feeds two 33/11kV, 2 x 15 MVA and 1 x 15 MVA distribution substations. Dawaki feeder (line 3) also feeds GHE via a 1 x 15 MVA substation. These 15 MVA substations have eight numbers of 11 kV feeders (Fd) that powers the estate. The specification of the substation transformers and overhead lines are presented in Tables 1 and 2, respectively.

TABLE I.   SUBSTATION TRANSFORMERS

Substation Transformer	Specification		
	Power (MVA)	Voltage (kV)	Vector group
TR 1	60	132/33	Dyn11
TR 2	60	132/33	Dyn11
TR 3	15	33/11	Dyn11
TR 4	15	33/11	Dyn11
TR 5	15	33/11	Dyn11
TR 6	15	33/11	Dyn11

TABLE II.   OVERHEAD LINES

Overhead Lines	Specification				
	Length (km)	Voltage (kV)	Current capacity (A)	Impedance (Ω/km)	
				r	x
Line 1	11.4	132.0	1200.0	0.176	0.392
Line 2	15.0	33.0	600.0	0.015	0.300
Line 3	8.0	33.0	600.0	0.015	0.300

V. METHODOLOGY

HOMER and DIgSILENT software were used to carry out this study. The methodology was divided into a framework and implementation flow chart.

A. Methodology Framework

The methodology framework involved the following components: The load consumption, obtained from Abuja Electricity Distribution Company (AEDC), renewable energy resource potential, assessed from National Aeronautics and Space Administration (NASA) in HOMER and the distribution network parameters of Gwarinpa housing estate. These parameters were the input for HOMER optimization that produced the optimum system. DIgSILENT was used to conduct a load flow analysis to investigate the impact of wheeling renewable DG on the distribution network.

B. Methodology Implementation Flow Chart

The implementation process shown in Fig. 6 was followed.
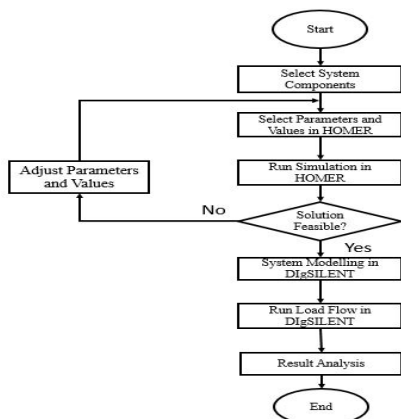

Fig. 6.   The methodology implementation flow chart

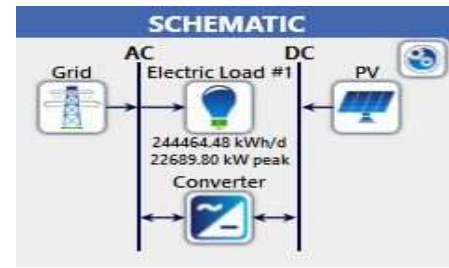The resultant system schematic designed in HOMER is shown in Fig. 7.

Fig. 7.   Schematic design in HOMER

VI. RESULTS AND DISCUSSION

(1) THE DISTRIBUTION NETWORK PARAMETERS

The load flow conducted on the existing distribution network produced the following result:

A. Voltage Profile

The result showed the lowest voltage of 0.94 p.u on buses 7 and 8. Bus 4 had a lower limit voltage of 0.95 p.u, as shown in Fig. 8. This result formed the basis for connecting the DG.
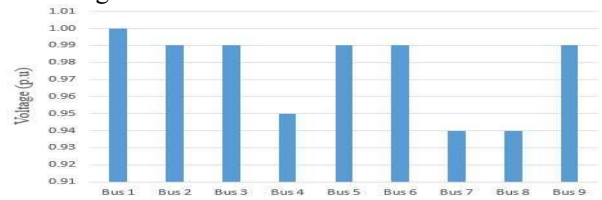

Fig. 8.   Bus voltage profile of the distribution network.

B. Fault level

The short circuit current was significant on bus 1, with a value of 43.74 kA. Bus 2 and 5 also recorded significant 30.90 and 21.66 kA, respectively, as shown in Fig. 9.
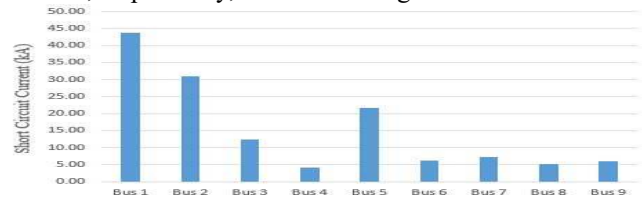

Fig. 9.   Short circuit current of the distribution network.

C. Lines losses

Both the active and reactive power losses were ascertained and presented in Fig. 10. Line 2, which was 81.26 % loaded, exceeded the maximum loading of 80 %. Thus, recorded high losses.
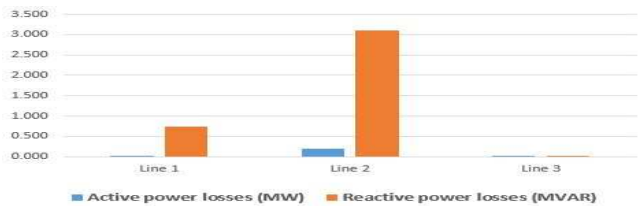

Fig. 10.   Active and Reactive power losses of the distribution network.

D. Thermal loading

The percentage loading of the network equipment is shown in Fig. 11. Line 2 was 81.26 % loaded, beyond the maximum allowable 80 %.
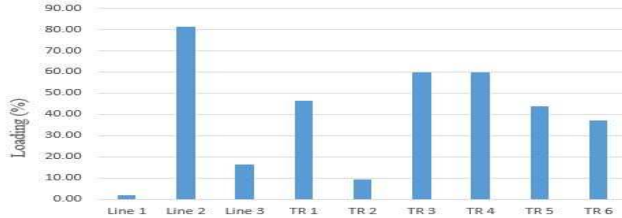

Fig. 11.   Thermal loading of the distribution network.

(2) THE IMPACT OF DG ON THE DISTRIBUTION NETWORK PARAMETERS

The connection of the DG (PV system) to the distribution network was carried out in two different scenarios. For each scenario, the impact of the connected DG on voltage profile, fault level, line losses and thermal loading were ascertained. The PV systems and specifications are presented in Table III.

TABLE III.   PV SYSTEMS

PV System	Specification			
	Active power (kW)	*No. of parallel inverter*	*Local controller*	*Output power (kW)*
PV	1875	10	Voltage	18750
PV(1)	1875	5	Voltage	9375
PV(2)	1875	5	Voltage	9375

A. Voltage Profile

- *First Scenario: PV system connected to buses 7 and 8*

PV systems denoted as PV and PV(1) were connected to buses 7 and 8, respectively. Expectedly, improvement in bus voltages was observed. The comparison made with the distribution network is shown in Fig. 12.
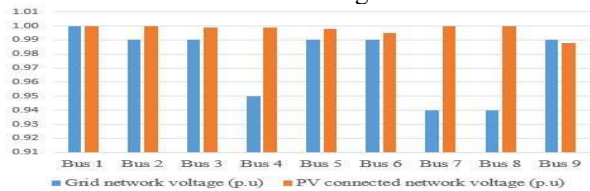

Fig. 12.   The comparison of the distribution network and the PV connected network.

- *Second Scenario: PV system connected to buses 7, 8 and 9*

Bus 7, 8 and 9 were connected with PV systems. PV (2) denotes the PV system connected to bus 9. The result obtained and the comparison with the grid distribution network is shown in Fig. 13. This scenario produced a great improvement in all the buses.
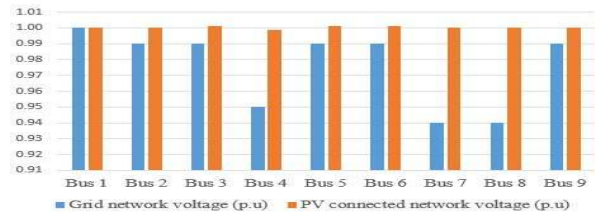

Fig. 13.   The comparison of the distribution network and the PV connected network.

B. Fault Level

The impact of the PV systems connected to the distribution network based on the two scenarios was determined. The results obtained were compared with the grid distribution network for evaluation.

- *First Scenario: PV system connected to buses 7 and 8*

The impact of the connected PV system on the fault level of the distribution network was negligible, as shown in Fig. 15. For the second scenario, the result obtained showed no deviation from the first scenario. Thus, the result of the second scenario was not presented to avoid repetition.
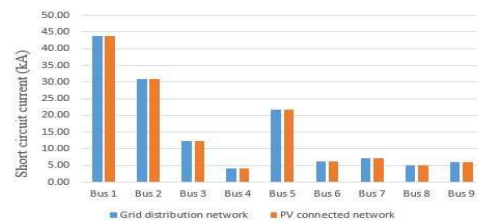

Fig. 15.   The impact of connecting PV system to bus 7 and 8 on the fault level of the distribution network.

C. Line Losses

- *First Scenario: PV system connected to bus 7 and 8*

The active and reactive power losses were determined and presented in Fig. 16. The erstwhile high losses seen on line 2 of distribution network (Fig 10) was drastically minimized.
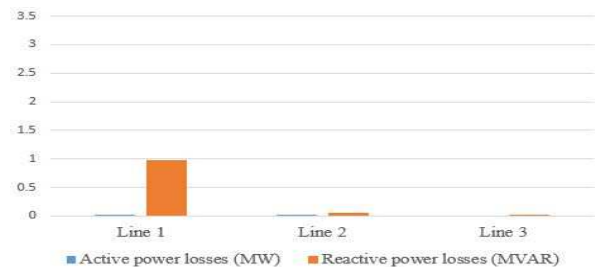

Fig. 16.   The impact of connecting PV system to bus 7 and 8 on the distribution network losses.

- *Second Scenario: PV system connected to buses 7, 8 and 9*

The result obtained is shown in Fig. 17. Lines losses were significantly minimized with the integration of the PV system to the distribution network.
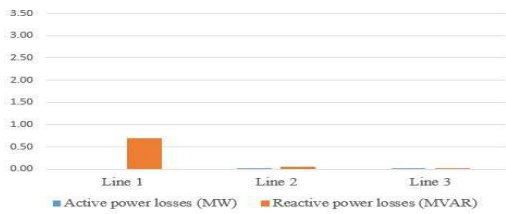
Fig. 17. The impact of connecting PV system to bus 7, 8 and 9 on the line losses of the distribution network.

D. Thermal Loading

The impact on the network loading was determined, and comparisons were made with the distribution network.

- *First Scenario: PV system connected to buses 7 and 8*

The PV systems were sufficiently loaded in order to determine the impact on the network. From the of Fig. 19, the equipment loading was significantly minimized.
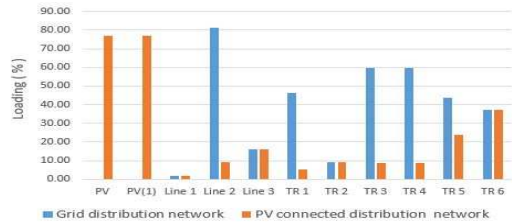

Fig. 19. The impact of connecting PV systems to buses 7 and 8 on thermal loading of the distribution network.

The overloaded line 2 was drastically reduced. The loading dropped from over 80 % to less than 10 %, with additional capacity created by the integration of PV systems.

- *Second Scenario: PV system connected to buses 7, 8 and 9*

The result obtained is shown in Fig. 20. The connected PV systems brought about a reduction in the thermal load of the equipment.
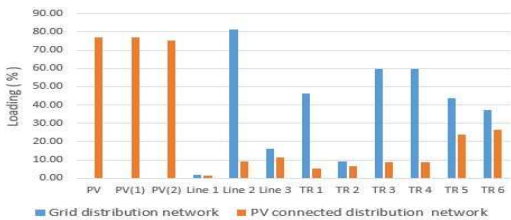

Fig. 20. The impact of connecting PV systems to buses 7, 8 and 9 on thermal loading of the distribution network.

VII. CONCLUSION

In this paper, a 9-bus grid distribution network was used to assess the impact of wheeling renewable distributed generation on residential load. HOMER and DIgSILENT simulation software was used to determine the potential resources for renewable energy and the impact of wheeling DG to the load on voltage profile, fault level, line losses and thermal loading of the grid distribution network, respectively. Various DG connection scenarios were tested, and results were obtained. Based on the result obtained, the following conclusion was drawn:

- The voltage profile of the network improved with the connection of DG. Bus 7 and 8 that erstwhile had 0.94p.u significantly improved with the lowest voltage value of 0.99p.u.

- The fault level of the grid distribution network was insignificant with the introduction of DG to the network. Though, this is largely due to inverter-based DG used.

- The grid distribution line losses were significant, particularly on line 2. The reactive power loss was 3.15 MVAR but drastically reduced to 0.13 MVAR with the connection of DG. Losses in other lines were also improved.

- DG creates additional capacity to the load and therefore reduces the loading of the existing network components. The thermal loading of the overloaded line 2 dropped from 81.26 % to less than 10 %. Other equipment also had improvement in thermal loading.

References

[1] S. Olanrewaju, S. Olafioye, and E. Oguntade, "Modelling Nigeria Population Growth: A Trend Analysis Approach," *International Journal of Innovative Science and Research Technology,* vol. 5, pp. 52-64, 2020.

[2] K. Kavaklioglu, "Principal components based robust vector autoregression prediction of Turkey's electricity consumption," *Energy Systems,* vol. 10, pp. 889-910, 2019.

[3] K. Olaniyan, B. McLellan, S. Ogata, and T. Tezuka, "Estimating residential electricity consumption in Nigeria to support energy transitions," *Sustainability,* vol. 10, p. 1440, 2018.

[4] W. N. Murray, "Energy wheeling viability of distributed renewable energy for industry," Cape Peninsula University of Technology, 2018.

[5] H. Quan, B. Li, X. Xiu, and D. Hui, "Impact analysis for high-penetration distributed photovoltaic generation integrated into grid based on DIgSILENT," in *2017 IEEE Conference on Energy Internet and Energy System Integration (EI2),* 2017, pp. 1-6.

[6] T. M. Azerefegn, R. Bhandari, and A. V. Ramayya, "Techno-economic analysis of grid-integrated PV/wind systems for electricity reliability enhancement in Ethiopian industrial park," *Sustainable Cities and Society,* vol. 53, p. 101915, 2020.

[7] H. M. Al Ghaithi, G. P. Fotis, and V. Vita, "Techno-economic assessment of hybrid energy off-grid system—A case study for Masirah island in Oman," *Int. J. Power Energy Res,* vol. 1, pp. 103-116, 2017.

[8] T. Al Momani, A. Harb, and F. Amoura, "Impact of photovoltaic systems on voltage profile and power losses of distribution networks in jordan," in *2017 8th International Renewable Energy Congress (IREC),* 2017, pp. 1-6.

[9] H. M. Sultan, A. A. Z. Diab, O. N. Kuznetsov, Z. M. Ali, and O. Abdalla, "Evaluation of the impact of high penetration levels of PV power plants on the capacity, frequency and voltage stability of Egypt's unified grid," *Energies,* vol. 12, p. 552, 2019.

[10] A. T. Dahiru and C. W. Tan, "Optimal sizing and techno-economic analysis of grid-connected nanogrid for tropical climates of the Savannah," *Sustainable Cities and Society,* vol. 52, p. 101824, 2020.